Hindawi
Geofluids
Volume 2022, Article ID 5383257, 15 pages
https://doi.org/10.1155/2022/5383257

WILEY | Hindawi

Research Article

Analysis of Surface Deformation and Settlement Characteristics Caused by Tunnel Excavation and Unloading

Xinfeng Wang,[1] **Shan Li**,[2] **Youyu Wei**,[1] **and Yiying Zhang**[1]

[1]*School of Environment and Resources, Xiangtan University, Xiangtan, Hunan 411105, China*
[2]*School of Qilu Transportation, Shandong University, Jinan, Shandong 250002, China*

Correspondence should be addressed to Xinfeng Wang; wangxinfeng110@126.com

Received 8 February 2022; Accepted 14 March 2022; Published 30 March 2022

Academic Editor: Hailing Kong

Aiming at the problems of surface deformation and unloading settlement caused by urban tunnel construction, the basic characteristics of surface deformation caused by tunnel construction, the main influencing factors of surface deformation and settlement, and the temporal and spatial evolution law of stress field and displacement field of surface deformation and settlement are studied by using the comprehensive methods of evaluation factor analysis, theoretical research, and numerical simulation. The results show that the surrounding rock deformation of the tunnel is mainly concentrated in the arch crown and arch bottom, and the deformation gradually decreases from the center of the tunnel to the periphery. The surrounding rock of arch crown has sudden settlement, large deformation rate and amount, and poor stability of surrounding rock, and is prone to engineering accidents such as block falling and even collapse. The farther away from the tunnel, the smaller the degree of settlement. As the time step of tunnel excavation increases, the influence area of surface deformation and settlement increases gradually. After the tunnel adopts reasonable lining support, it can effectively prevent soil deformation transmission and restrain tunnel instability deformation, so as to prevent surface deformation and settlement by improving the self stability of surrounding rock and taking lining support and other measures.

1. Introduction

With the rapid development of China's economy, the level of urbanization is also in the stage of rapid development, followed by a series of urban syndrome phenomena, such as oversaturated urban population and congested building space. Rational and effective use of underground space can solve the problem of urban syndrome. Urban tunnel construction can well solve the contradiction between urban construction and lack of land resources, effectively promote urban sustainable development, and accelerate the process of urban modernization while protecting the environment [1]. However, the construction of urban tunnels will destroy the surrounding soil to a certain extent, and the soil will be disturbed by excavation, resulting in soil instability and deformation, which will lead to inclined deformation, tensile cracking, compression deformation, and even collapse of ground buildings. Therefore, it is of great significance to study the surface deformation and environmental damage caused by urban tunnel construction. The model establishment and settlement research on the surface deformation and settlement characteristics caused by urban tunnel construction will provide a scientific theoretical basis for the rational design of tunnel construction and the protection of surrounding buildings.

The construction methods of urban tunnels are divided into open excavation method and concealed excavation method. The construction methods of urban tunnels are restricted by the hydrogeological conditions, engineering properties, surrounding obstacles, economy and environmental protection, construction period, and quality requirements of the excavation project. There are various construction methods of urban tunnels. With the development and progress of urban underground tunnel construction in China, its own construction technology is also developing and improving. New construction methods are emerging, and the level of construction technology is gradually improved. Considering the safety and convenience of tunnel construction, shield method and shallow buried excavation method are mostly

used at present. Peck first put forward the estimation formula of ground lateral settlement during shield tunnel construction in 1969 [2]. Peck formula has been widely used because of its simple usage. However, in the actual engineering practice, peck formula cannot be used for detailed analysis. In the later stage, many experts at home and abroad revised and improved peck formula according to the actual situation. Y. Shao used peck empirical formula and FLAC3D to establish a numerical simulation model to predict the land settlement caused by shield construction of Suzhou Metro Line 4 [3]. Y. Fan and others demonstrated the feasibility of numerical simulation of construction process with finite element tunnel model based on the measured data [4]. For the restrictive factors affecting the amount of land settlement, J. Jia and others studied the influence law of different construction methods on land settlement [5], focusing on the deformation and failure of surrounding rock mass caused by tunnel excavation and unloading, Mohr-Coulomb criterion, Griffith strength criterion, Murrell strength criterion, Drucker Prager criterion, Hoek Brown criterion, Mises criterion, double shear strength theory, unified strength theory, stress catastrophe theory Fuzzy strength theory, maximum stress-strain theory, s criterion, y criterion, t criterion, J-integral criterion, maximum energy release rate criterion, and test criterion [6–10]. In terms of surrounding rock failure criteria under dynamic load, the most widely used are stress and strain strength criteria, energy strength criteria, damage failure criteria, and empirical failure criteria [11–14]. With the wide application of the strength failure criterion of rock and soil mass in tunnel excavation under dynamic and static loads, it can explain and judge the fracture behavior of disturbed rock mass, especially the application of energy dissipation theory and acoustic emission loading experiment, and reveal the deformation and failure law of tunnel rock mass to a certain extent [15, 16].

Based on the above literature research, the surface deformation caused by tunnel excavation has always been the focus of current research, which needs to be further studied. Based on the engineering background of urban tunnel construction, the author focuses on the deformation of ground surface under the disturbance of tunnel excavation and temporal and spatial evolution law of rock and soil settlement and failure, analyzes the main factors affecting the unloading instability and deformation of excavated rock mass, and lays a solid foundation for the safety, stability, prevention, and control of urban tunnel construction.

2. Characteristics of Surface Deformation Caused by Urban Tunnel Construction

2.1. The Effect Characteristics of Surface Deformation. Land subsidence does not occur at one time. A large number of engineering practices show that land subsidence occurs in stages, and there will be different forms of deformation in each time period, and the magnitude of settlement is also different. According to the time sequence, the deformation experience can be divided into early deformation, deformation during construction, and subsequent deformation. The time effect characteristic curve is shown in Figure 1. In the early deformation stage, when the surface deformation is monitored, but the heading face does not reach the position of the surface monitoring point, due to the insufficient support capacity of working face and other reasons, the soil movement trend before work is backward and downward, and the surface sinks slightly. Taking shield construction as an example, the deformation in the construction stage is mainly caused by soil loss and positive additional thrust without considering soil drainage. Due to the influence of tunnel excavation, the stratum around the tunnel will inevitably move. On the one hand, it is impossible to support the surrounding soil immediately after tunnel excavation; on the other hand, the support cannot completely prevent formation deformation. At this stage, the surface will sink significantly. In the subsequent deformation stage, the tunnel settlement shows a dynamic development state. After the tunnel excavation, the surface settlement still shows an increasing trend for a long time, sometimes even more than a few years.

Studying the time-dependent characteristics of long-term surface settlement caused by tunnel excavation can study the variation of maximum settlement with time and the variation of width coefficient of long-term settlement tank with time [17–18]. The width coefficient of long-term settlement tank is a function of time and will change with time and consolidation settlement. With the passage of time, the maximum subsidence and width coefficient will continue to increase.

2.2. Spatial Effect Characteristics of Surface Deformation. The rock movement caused by tunnel construction is three-dimensional in space and changes with the advance of tunnel working face. With the longitudinal development of tunnel, the surface settlement trough continues to expand and develop. The spatial movement of strata is shown in Figure 2. Rock movement starts from the excavation face of the tunnel and extends to the front, upper part, and upper part of the side. From bottom to top, its influence range gradually expands and is diffuse. The distance from the working face of the tunnel affects the displacement of the vertical stratum, and the largest settlement occurs in the vault area, forming a "settlement trough" in the horizontal direction. The farther away from the excavation face, the settlement decreases and attenuates gradually, the shape of the settlement tank becomes deeper and narrower, and the width of the settlement tank becomes smaller and smaller. The settlement profile of the settlement tank is conical, and the cone faces the direction of the tunnel. The contour line will also extend forward with the excavation. The surface settlement is symmetrically distributed. The position with the largest surface settlement is directly above the tunnel axis, and the settlement begins to decrease to the left and right.

According to the characteristics of spatial effect, the deformation of soil during shield construction is shown as the trend of horizontal movement of soil around the tunnel when the shield passes through the tunnel; the settlement trough is normally distributed, and the settlement is symmetrically distributed. The maximum settlement is directly above the axis of the tunnel. The settlement of the soil above the tunnel increases with the deepening of the tunnel, and the settlement reaches the maximum near the top of the tunnel lining. The soil below the tunnel has upward displacement and is in uplift state, with the maximum value at the bottom of the tunnel lining.

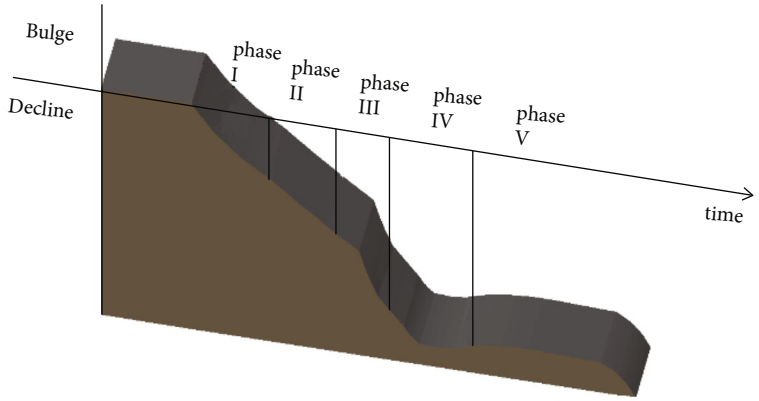

Figure 1: Time effect characteristic curve.

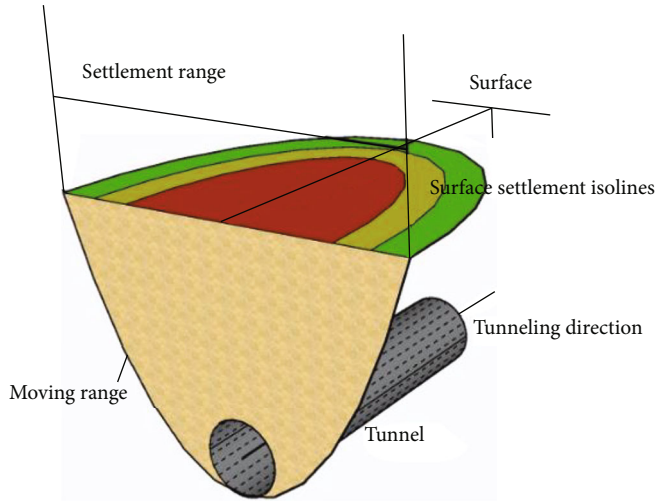

Figure 2: Spatial pattern of stratum deformation.

2.3. Scale Effect Characteristics of Surface Deformation. Peck first proposed the estimation of land settlement to measure the deformation and settlement of soil.

$$S(x) = S_{\max} e^{-\frac{x^2}{2i^2}}, \tag{1}$$

$$S_{\max} = \frac{V_{\text{loss}}}{i\sqrt{2\pi}}. \tag{2}$$

In formula ((1)–(2)), $S(x)$ is the land settlement, m; x is the horizontal coordinate, m; $S_{\max}$ is the maximum settlement, m; V_{loss} is the loss of soil mass, m^3/m; i is the width coefficient of settlement tank, m.

$$i = R\left(\frac{z_0}{2R}\right)^n = Kz_0. \tag{3}$$

In formula (3), R is the outer radius of the tunnel, m; z_0 is the buried depth of the tunnel, m; n =0.8~1.0, the softer the soil, the greater the n value; K is the width parameter of sedimentation tank.

Formation loss rate V_l under the premise of no drainage, the formula of maximum displacement and formation loss is as follows:

$$S_{\max} = \frac{AV_l}{i\sqrt{2\pi}}. \tag{4}$$

Taking the tunnel with circular section as an example, the engineering formula for estimating land settlement is:

$$S = \left[\frac{0.313V_lD^2}{Kz_0}\right] \exp\left[\frac{-x^2}{2K^2z_0^2}\right]. \tag{5}$$

The size effect of settlement can be measured by the formation loss rate V_l and the width coefficient K of the sedimentation tank. V_l determines the value of settlement, K determines the width coefficient of settlement tank, and then affects the curve shape of settlement tank, such as wide and shallow. And there is a linear relationship between V_l and K [19].

Attewell et al. put forward the estimation formula of longitudinal ground settlement above the tunnel axis:

$$S(y) = S_{\max}\left[\Phi\left(\frac{y-y_i}{i}\right) - \Phi\left(\frac{y-y_f}{i}\right)\right]. \tag{6}$$

In formula (6), $S(y)$ is the land settlement, m; y is the surface point coordinate, m; y_i is the starting point of propulsion, m; y_f is the current position, m.

By analyzing the settlement value of soil above the center line of the tunnel, Jiang Xinliang obtained the formula of settlement tank coefficient at different depths:

$$\begin{gathered} S_z(x) = S_{\max}\exp\left[-\frac{x^2}{2iz^2}\right], \\ S_{\max}(z) = S_{\max}(1-z/h)^{-0.3}, \\ i(z) = i(1-z/h)^{0.3}. \end{gathered} \tag{7}$$

In the construction of shallow buried tunnel, the scale effect of ground deformation and settlement caused by the shrinkage of section caused by the movement of soil around the tunnel can be measured by the following formula, that is, the difference of ground settlement caused by the change of excavation range:

$$\begin{gathered} W(X) = W_{\Omega}(X) - W_{\omega}(X), \\ W(X) = \iint_{\Omega-\omega}\frac{\tan\beta}{\eta}\exp\left[-\frac{\pi\tan^2\beta}{\eta}(X-\varepsilon)^2\right]d\varepsilon\, d\eta. \end{gathered} \tag{8}$$

Similarly, with the help of superposition principle, the calculation formula of ground horizontal displacement is obtained:

$$\begin{gathered} U(X) = U_{\Omega}(X) - U_{\omega}(X), \\ U(X) = \iint_{\Omega-\omega}\frac{(X-\varepsilon)\tan\beta}{\eta^2}\exp\left[-\frac{\pi\tan^2\beta}{\eta}(X-\varepsilon)^2\right]d\varepsilon\, d\eta. \end{gathered} \tag{9}$$

The scale effect of surface deformation can also be measured by using the formulas of surface curvature deformation, horizontal deformation, and slope deformation.

3. Analysis on Influencing Factors of Surface Deformation Caused by Urban Tunnel Construction

3.1. Analysis of Influencing Factors of Surface Deformation. The surface deformation caused by the construction of urban shallow underground engineering is related to the urban natural environment, geological conditions, construction methods and technologies (tunnel buried depth, tunnel section size), and other factors. The influencing factors of surface subsidence are divided into internal factors (formation conditions, changes of groundwater, thickness of overburden) and human factors (design and construction factors).

The influence of soil characteristics means that the rearrangement of soil particles will affect the surface deformation. Geological characteristics are important factors affecting surface deformation. When the direction of the tunnel is the same as the direction of the fold, rock slide is easy to occur in the building. Urban tunnels are easy to collapse when passing through fault zones, and ground buildings are easy to produce uneven settlement. The influence of soil properties on surface settlement can be considered from soil parameters. The experimental results show that the increase of elastic modulus, cohesion, Poisson's ratio, and internal friction angle of soil will reduce the surface settlement to varying degrees.

Previous research shows that the depth of decline of formation water level is directly proportional to land subsidence [20]. When the rock is wetted by water, the particle surface inside the rock will change, and the rock strength will decrease, resulting in increased movement between rock layers. The softening effect is closely related to the properties of rocks, and the softening effect of formation water on high-strength crystalline rocks is small. Confined water reduces the effective normal stress and potential shear resistance. The lubrication effect is reflected in the reduction of friction resistance and water pressure, which leads to the reduction of normal stress and reduces the shear strength of rock. The change of seepage field leads to the change of rock and soil stress. When a large amount of groundwater in the tunnel is drained, the pore water pressure of saturated soil decreases, and the range of negative pore pressure in unsaturated area increases, resulting in the increase of effective stress. The seepage direction of water is downward. With the increase of effective stress, new settlement of soil will occur, and groundwater seepage will expand the range of surface deformation [21, 22].

There are many factors that affect the surface deformation in the process of urban tunnel construction, but they are ultimately related to the in situ stress release value. With the increase of in situ stress release on the excavation surface, the surface settlement will increase obviously, and the deformation of arch bottom, arch crown, and arch waist on the tunnel excavation surface will also increase. The plastic zone of surrounding rock is also increasing, and the stability of surrounding rock is destroyed, from stable state to unstable state. According to the theory of stress release and formation loss, the stress release rate is obtained with the help of numerical simulation and theoretical calculation. With the increase of stress release coefficient, the surface displacement directly above the tunnel axis shows an increasing trend and increases in a parabola. The law of surface settlement can be obtained by analyzing the width coefficient of settlement tank.

3.2. Fishbone Diagram Analysis of Surface Deformation Caused by Shield Construction. Causality diagram or characteristic factor diagram is used to analyze the causality between characteristic results and factors that may affect the results. Many possible causes can be summarized into cause categories and sub causes. Draw a figure similar to fish bone, so this tool is also called fishbone diagram. All the listed problems are classified according to the 5 m factor method and marked on

the fishbone diagram (5 m method: five factors: man, machine, material, method, and milieu). Through the fishbone diagram analysis method, the research problems and causes are clearly and intuitively displayed on a diagram, which can help researchers quickly find out the problems and formulate corresponding countermeasures.

At the beginning of excavation, the soil outside the slip surface is consolidated and settled due to the groundwater level. The soil in front is compacted, the pore pressure dissipates, and the compression modulus increases, resulting in settlement. After the shield is implemented, the surrounding soil is unloaded and the pressure on the excavation surface is too large, resulting in stratum uplift [23]. When the shield passes through, the soil settlement is caused by the friction shear force in the process of correcting the deviation when the shield machine moves backward, heads up or heads down. After the shield passes through, the rear clearance will increase, which will cause settlement and soil disturbance. Finally, a longer continuous settlement time. Soil loss refers to the soil loss caused by the building gap after soil excavation, unloading, and shield tail penetration. Frontal additional thrust refers to the support force provided by applying frontal thrust to maintain a stable excavation surface. However, when there are unknown obstacles in front of the excavation face, when the excavation face stops working for a long time, when it is pushed again, when the machine head passes through the interface of different soil layers, it is likely to produce large changes in the front propulsion force, and then the soil mass will have the soil squeezing effect of ground uplift before excavation and ground settlement after excavation. The friction between shield shell and soil is the friction generated by the relative movement between the soil and the contact surface of shield machine. After receiving the friction, the surrounding soil will move, resulting in soil deformation.

Taking the surface deformation caused by shield construction as the main bone and the personnel, materials, construction technology, mechanical equipment, and environment as the big bone, the fishbone diagram is drawn through the system safety analysis method, as shown in Figure 3. Among them, the selection of grouting materials is related to the amount of ground settlement, while high-strength materials cause less ground settlement. Grouting materials generally need materials with excellent properties and reasonable proportion. The construction technology can be considered from the aspects of tunnel buried depth, excavation radius, grouting process, shield machine propulsion speed, and so on. When the buried depth of the tunnel is relatively shallow, the soil settlement of surface deformation decreases with the increase of the buried depth of the tunnel, showing a linear relationship. When the buried depth of the tunnel increases to a certain value, the settlement tends to be stable. And the relationship between surface settlement and section size is that the settlement increases with the increase of tunnel section diameter [24]. Whether the backfill grouting is timely or not will affect the displacement and deformation of the surrounding soil towards the tunnel. The grouting process shall be controlled considering the grouting pressure, capacity, time, and radius. Control the propulsion speed, and select different propulsion speeds under different geological conditions to prevent the soil from being squeezed as much as possible. When the shield must stop moving forward, measures must be taken to prevent the shield from retreating, and the head and tail of the shield should be tightly sealed to reduce the impact on soil deformation during shutdown. The parameters and types of mechanical equipment, i.e., shield, determine its adaptability to the stratum, which is directly related to the stability of the excavation surface and the control of excavated volume. Therefore, the design and layout of cutter head and cutter and the selection of screw conveyor are the focus of research. Environmental factors mainly include the characteristics of soil itself, such as water content, permeability, flow plasticity, and the influence of groundwater on soil deformation.

4. Evolution Law of Surface Deformation and Settlement

4.1. External Evolution Law of Rock Mass in Tunnel Excavation

(1) Numerical model construction

In a shallow tunnel project in a city, the material mechanical parameters of soil are set for tunnel excavation. The original stress is self gravity field, and the tunnel diameter is 2 m. The method of full face excavation, excavation, and support is simulated, and 1/4 of the soil is selected for simulation. This excavation is divided into two times, and the support is established every 1 m. The support method is to spray concrete with a thickness of 0.2 m (elastic modulus of 10.5 GPa and Poisson's ratio of 0.25). The establishment model is shown in Figure 4.

(2) Evolution law of stress field

Analyze the horizontal stress nephogram and vertical stress nephogram of one excavation step (a), two excavation steps (b), two excavation steps and one support step (c). The horizontal stress nephogram is shown in Figure 5. The vertical stress nephogram is shown in Figure 6.

According to the analysis, the stress of surrounding rock around the tunnel is negative, indicating that they are in a state of pressure. Under horizontal stress, the central pressure of tunnel face is the largest; under the vertical stress, the pressure around the tunnel (arch waist) is the largest. According to the horizontal stress nephogram 5(a), 5(b), and 5(c), the tensile stress at the top of the one-step excavation model is 0.0274 MPa, 0.0283 MPa in two-step excavation, and 0.0277 MPa in two-step excavation with support, indicating that with the increasing stress on the tunnel excavation surface, the stress on the surrounding rock is relieved to a certain extent after lining support. According to the vertical stress nephogram and Figures 6(a)–6(c), the tensile stress at the top of the one-step excavation model is 0.0275 MPa, 0.0282 MPa in two-step excavation, and 0.0278 MPa in two-step excavation with support. From 6 (a) and 6(b), with the excavation of the tunnel, the force on the surface soil is increasing; According to 6(b) and 6 (c), the stress is relieved to a certain extent after the shotcrete lining support.

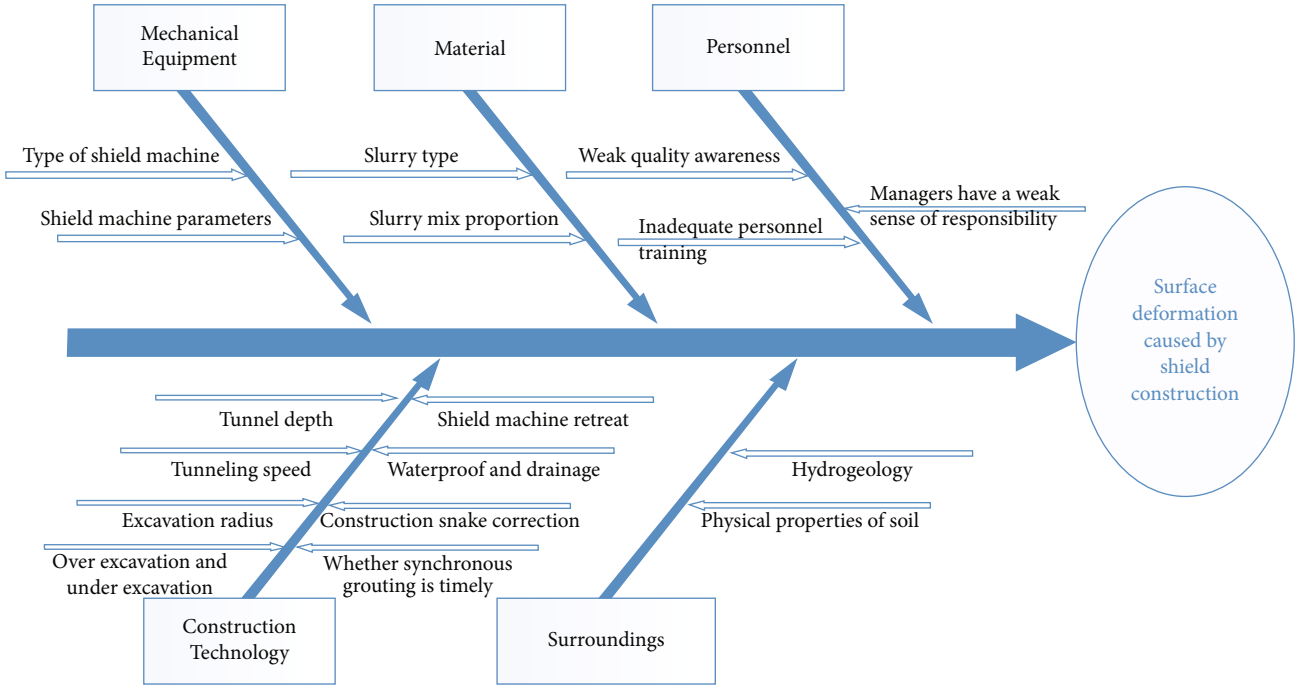

Figure 3: Analysis of surface deformation fishthorn method.

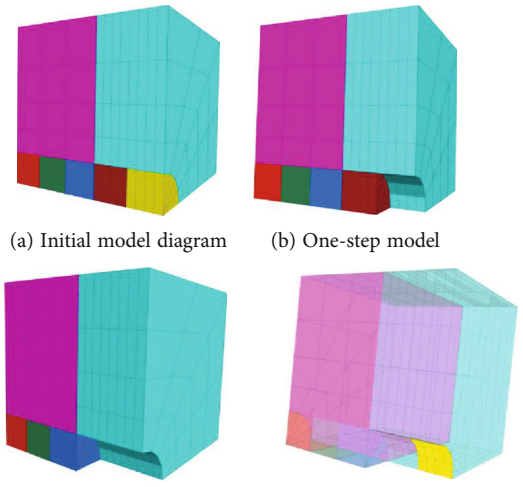

(a) Initial model diagram (b) One-step model

(c) Two-step model (d) Lining support model diagram

Figure 4: Model diagram.

(3) Displacement deformation law

The most obvious feature of surface deformation and settlement is the change of displacement, so the research on displacement can see the law of soil deformation and settlement caused by urban tunnel construction. Similarly, the total displacement nephogram, horizontal displacement nephogram, and vertical displacement nephogram of different excavation steps are analyzed to obtain their displacement and deformation characteristics, as shown in Figures 7–9.

According to the total displacement nephogram 7, the maximum deformation occurs at the vault. In one excavation step, the maximum displacement is 1.89 mm, in two excavation steps, 0.815 mm, and in one excavation two support step, the maximum displacement is 0.58 mm. According to the comparison between Figure 7(b) and Figure 7(c), the displacement of soil in the area of shotcrete is almost 0 mm, and the influence range of soil deformation tends to decrease. The displacement of the center of the tunnel face changes from 0.45 mm to 0.5 mm. By observing the horizontal displacement Cloud (Figure 8), it can be seen that the deformation affected area continues to extend with the advance of excavation, and the maximum horizontal displacement appears near the arch waist. It can be seen from Figures 8(b) and 8(c). After being

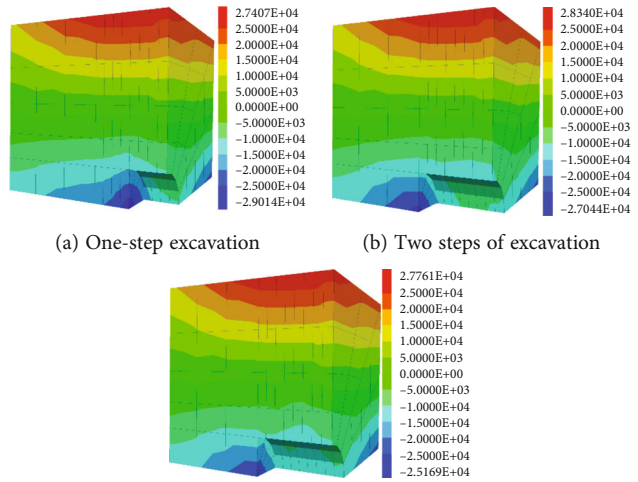

(a) One-step excavation (b) Two steps of excavation

(c) Two excavation steps and one support step

Figure 5: Horizontal stress nephogram.

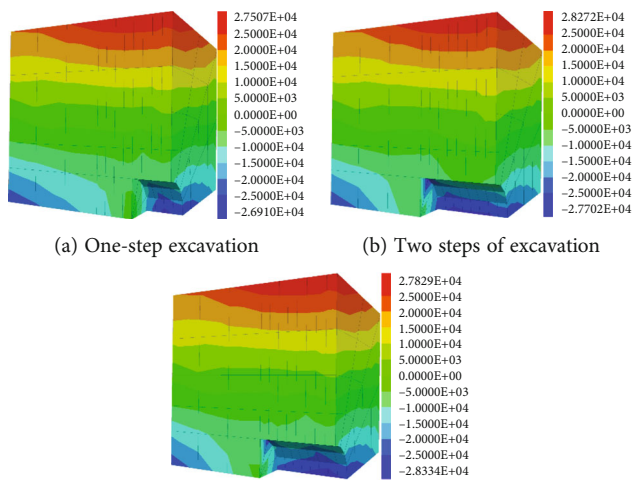

(a) One-step excavation (b) Two steps of excavation

(c) Two excavation steps and one support step

Figure 6: Vertical stress nephogram.

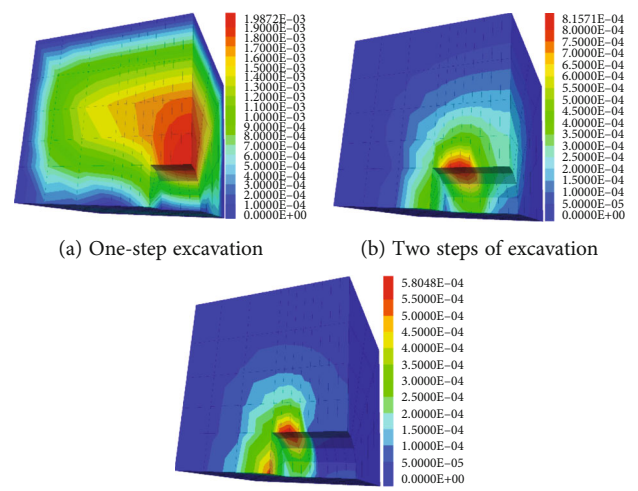

(a) One-step excavation (b) Two steps of excavation

(c) Two excavation steps and one support step

Figure 7: Total displacement cloud map.

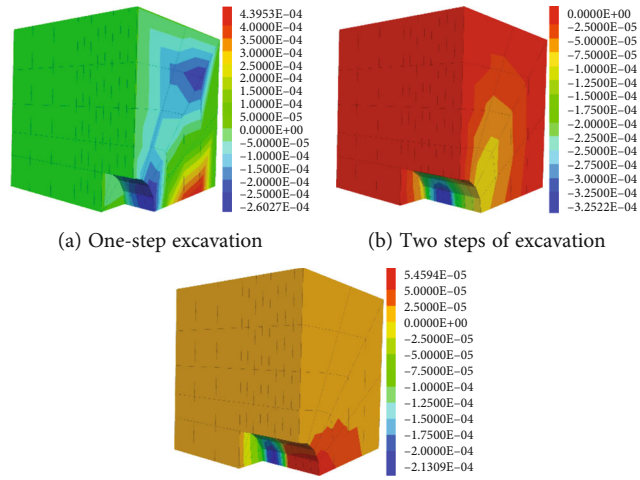

(a) One-step excavation (b) Two steps of excavation

(c) Two excavation steps and one support step

Figure 8: Horizontal displacement cloud map.

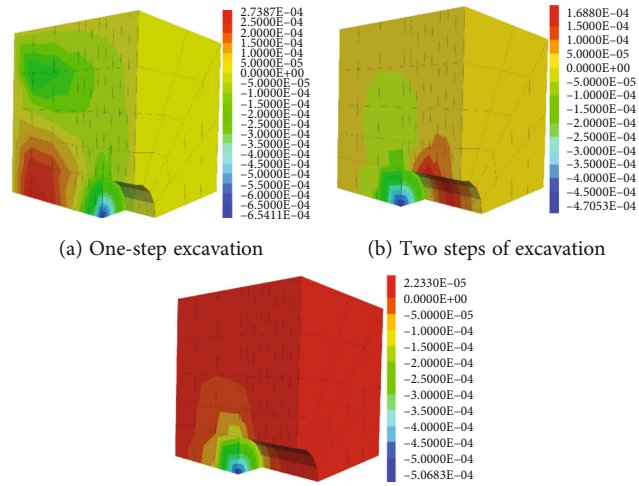

(a) One-step excavation (b) Two steps of excavation

(c) Two excavation steps and one support step

Figure 9: Vertical displacement cloud map.

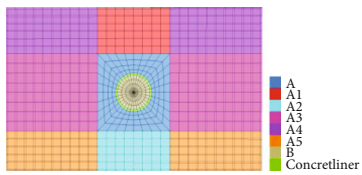

Figure 10: Tunnel grid.

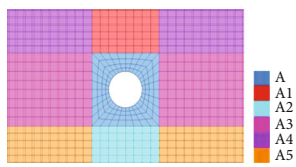

Figure 11: Model diagram after excavation.

supported by lining, the fluctuation range of horizontal displacement decreases, indicating that lining support blocks the propagation of deformation to a certain extent. According to the vertical displacement Cloud Figure 9, the negative displacement near the tunnel face is the largest. With the excavation, the displacement around the tunnel is increasing. It can be seen from Figures 9(b) and 9(c) that after the shotcrete is supported, the displacement tends to zero, indicating that reasonable support can control soil deformation and settlement within a certain range.

4.2. Internal Evolution of Excavated Rock Mass

(1) Numerical model construction

Firstly, considering the size of the model, the range of the soil block can be regarded as an infinite body. For the simulation, only one piece needs to be taken out of the infinite body for analysis and simulation. The excavation cross section of

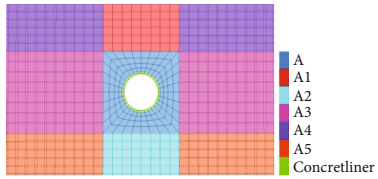

Figure 12: Model diagram after lining support.

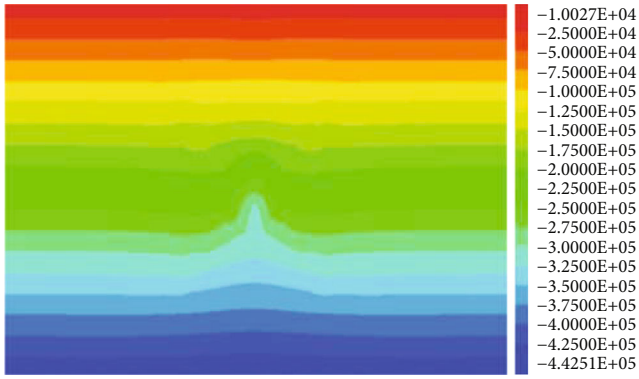

Figure 13: Initial vertical stress nephogram.

the selected tunnel is a circle with a diameter of 6 m. The deformation of soil caused by tunnel excavation is relatively large, so it is particularly important to select a reasonable boundary range. Consult the data to understand the influence scope of tunnel excavation. It is stipulated that the left and right boundaries are 3 times of the outer diameter of the tunnel, the buried depth of the tunnel is 10 m, and the bottom boundary is 1.5 times of the outer diameter of the tunnel. The whole calculation model is 25 m high and 42 m wide. After the simulated tunnel excavation, the lining support method is adopted, and the lining material is C30 concrete. Mohr-Coulomb constitutive model is generally used for mechanical calculation. The initial and boundary conditions of the model are to load the gravitational acceleration along the z-axis direction on the object with the initial density set, and to fix the command flow with no displacement and velocity on five surfaces.

Secondly, the cylindrical tunnel with peripheral radial grid, surrounding stratum, tunnel lining structure, and internal soil model are established to form a complete tunnel grid model. The establishment results of the circular tunnel grid and the formation grid around the tunnel are shown in Figure 10. Then, the gravity and displacement boundary conditions are applied and the material parameters are given to solve the self weight stress field. Next, in order to ensure the accuracy of the simulation and the correctness of the calculation, the displacement in the initial stress calculation is cleared and the rough hole is excavated. The model is shown in Figure 11. Finally, the tunnel support is simulated, and the elastic model is used to calculate the density, volume elasticity, and shear modulus of lining concrete. The model after excavation and support is shown in Figure 12, and the green area in the figure is lining.

(2) Evolution law of stress field

Add boundary conditions, give material parameters, and solve the self weight stress field. The stress nephogram under the initial stress field is shown in Figures 13 and 14. After the tunnel is excavated, the stress nephogram is shown in Figures 15 and 16. After the tunnel adopts lining support, its stress nephogram is shown in Figures 17 and 18.

Under the self weight stress field, the distribution of the stress field generally presents a horizontal strip distribution. In the area around the tunnel, there are changes and fluctuations due to the change of unit size, as shown in the middle part of Figure 13. Under the action of self weight stress field, the maximum vertical stress is -0.4425Mpa, according to the initial stress cloud diagram, which represents the compressive stress, as shown in Figure 13; the maximum horizontal stress is -0.2179 MPa, indicating compressive stress, as shown in Figure 14. The stress diagram after excavation is as follows: from Figure 15 to Figure 16, the maximum vertical stress and compressive stress are 0.4661 MPa, as shown in Figure 15; the maximum horizontal stress, tensile stress is 3.916 KPa and compressive stress is 0.2477 MPa, as shown in Figure 16. The stress nephogram after support is shown in Figure 17 to Figure 18. The maximum vertical stress, tensile stress is 1 KPa and compressive stress is 0.4524 MPa, as shown in Figure 17; the maximum horizontal stress is -0.2263 MPa, indicating compressive stress, as shown in Figure 18.

Before the tunnel is excavated, under the action of the initial stress field, it can be seen from the stress cloud Figure 13 that the surrounding rock is in a state of compression, so the stress and vertical stress in ZZ direction are negative. The compressive stress increases gradually from top to bottom. The ground deformation around the tunnel is large, and the place far from the tunnel tends to be balanced. After the tunnel is excavated, as shown in Figure 15, the stresses of the arch crown, arch bottom, and arch waist are negative and are in a state of pressure, of which the arch waist has the largest negative stress. After the lining support is adopted, as shown in Figure 17, a small range of simulated positive stress appears near the tunnel, that is, the red area represents the occurrence of tensile stress, and the tensile stress area appears within the support range, that is, the reinforcement and support of surrounding rock is reasonable and effective. The negative stress at the arch waist is the largest and diffuses outward from the two sides of the tunnel, and the stress becomes smaller, which is caused by the extrusion of lining support after the excavation of surrounding rock at this position.

(3) Displacement deformation law

The displacement nephogram under the initial stress field is shown in Figure 19. After the tunnel is excavated, its displacement nephogram is shown in Figure 20. After the tunnel adopts lining support, its displacement nephogram is shown in Figure 21. In Figures 19–21, the vertical displacement, horizontal displacement and total displacement are obtained.

Under the self weight stress field, the distribution of displacement field also presents a horizontal strip distribution, which fluctuates due to the change of element size in the

Figure 14: Initial horizontal stress nephogram.

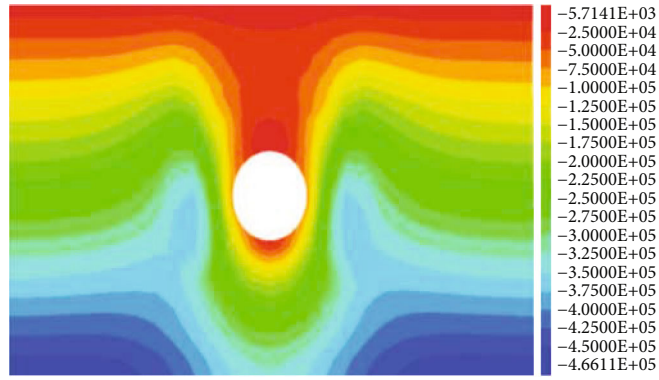

Figure 15: Vertical stress cloud after excavation.

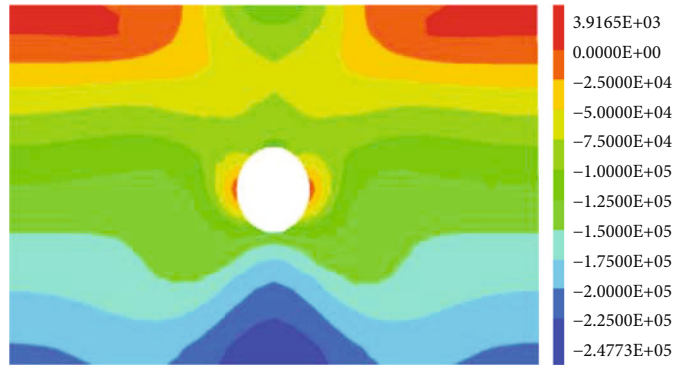

Figure 16: Horizontal stress cloud after excavation.

surrounding area of the tunnel. Under the action of self weight stress field, the maximum vertical deformation is -25.26 mm, and the direction is downward, indicating subsidence, as shown in Figure 19(a). The displacement change in the horizontal direction presents a "butterfly shape." The displacement after excavation is as follows: the maximum vertical displacement is about 38.40 mm, and the displacement at the vault is the largest, as shown in Figure 20(a); the maximum horizontal displacement is about 11.61 mm, which occurs at the left and right arch feet, as shown in Figure 20(b). The maximum vertical displacement after support is 24.87 mm at the vault, as shown in Figure 21(a); the maximum horizontal displacement after support occurs at the left and right arch feet, as shown in Figure 21(b). As shown in Figure 20, after the tunnel is excavated, the deformation around the tunnel is mainly concentrated in the arch crown and arch bottom. The deformation displacement decreases gradually around, the arch crown sinks and the

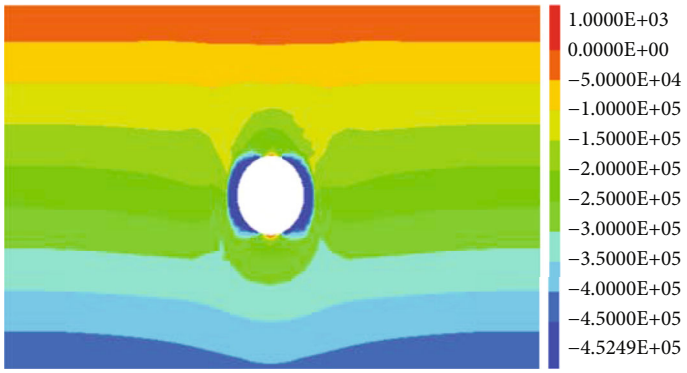

Figure 17: Vertical stress cloud after support.

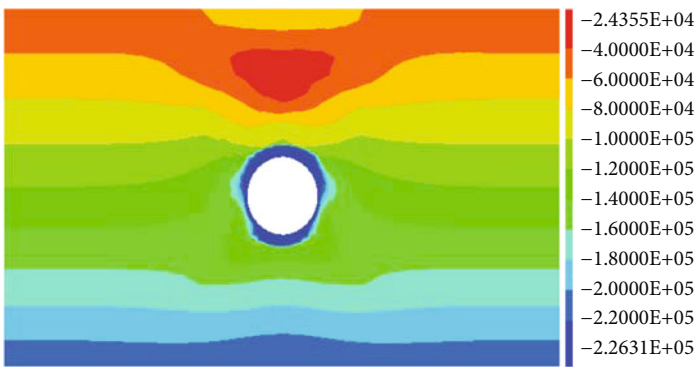

Figure 18: Horizontal stress cloud after support.

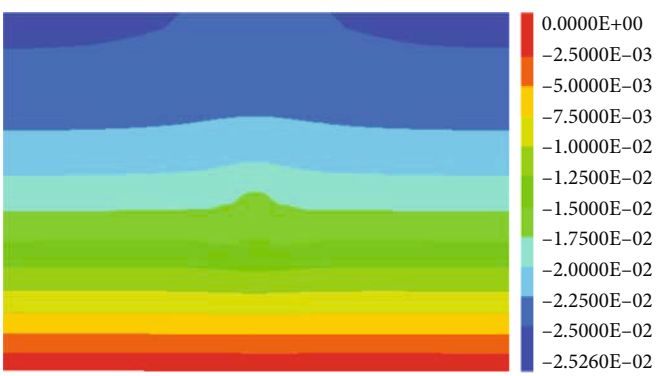

(a) Vertical displacement

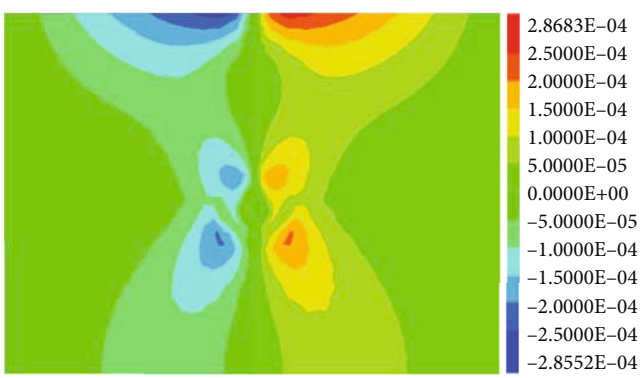

(b) Horizontal displacement

(c) Total displacement

Figure 19: Initial horizontal displacement nephogram.

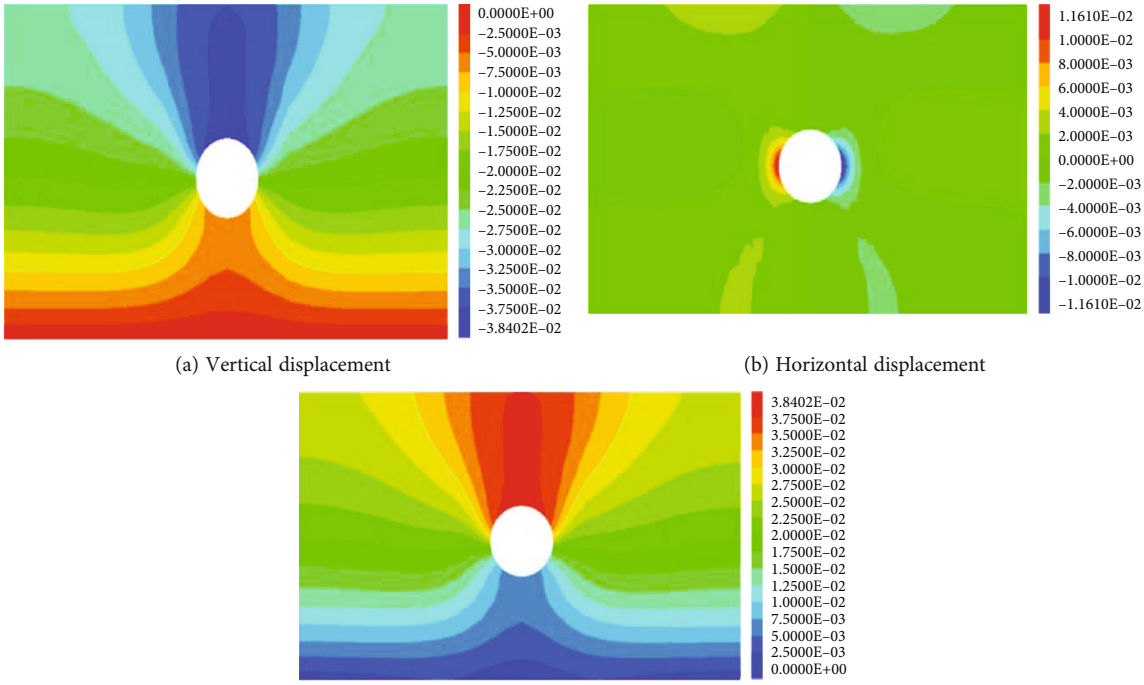

(a) Vertical displacement

(b) Horizontal displacement

(c) Total displacement

Figure 20: Displacement nephogram after excavation.

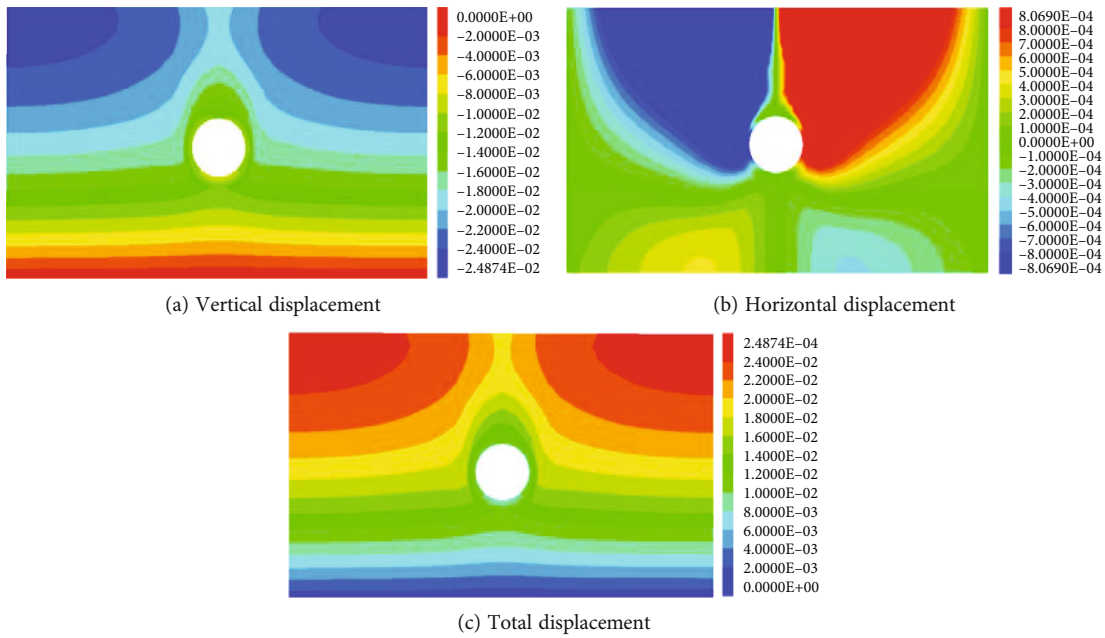

(a) Vertical displacement

(b) Horizontal displacement

(c) Total displacement

Figure 21: Displacement nephogram after support.

arch bottom bulges. As shown in Figure 20(a), the vertical displacement of the arch crown decreases by 38 mm and the arch bottom bulges by 7.5 mm. As shown in Figure 21 (a), the vertical displacement after support can be obtained. The arch crown drops by 10 mm and the arch bottom bulges by 7 mm. Therefore, reasonable support can alleviate surface deformation and settlement to a certain extent.

(4) Distribution law of plastic zone

The surrounding rock is in elastic zone, which means that the stress of each part limit value. When the stress in some areas of surrounding rock is greater than the strength limit, the plastic zone of surrounding rock is formed. The plastic zone after tunnel excavation can be divided into

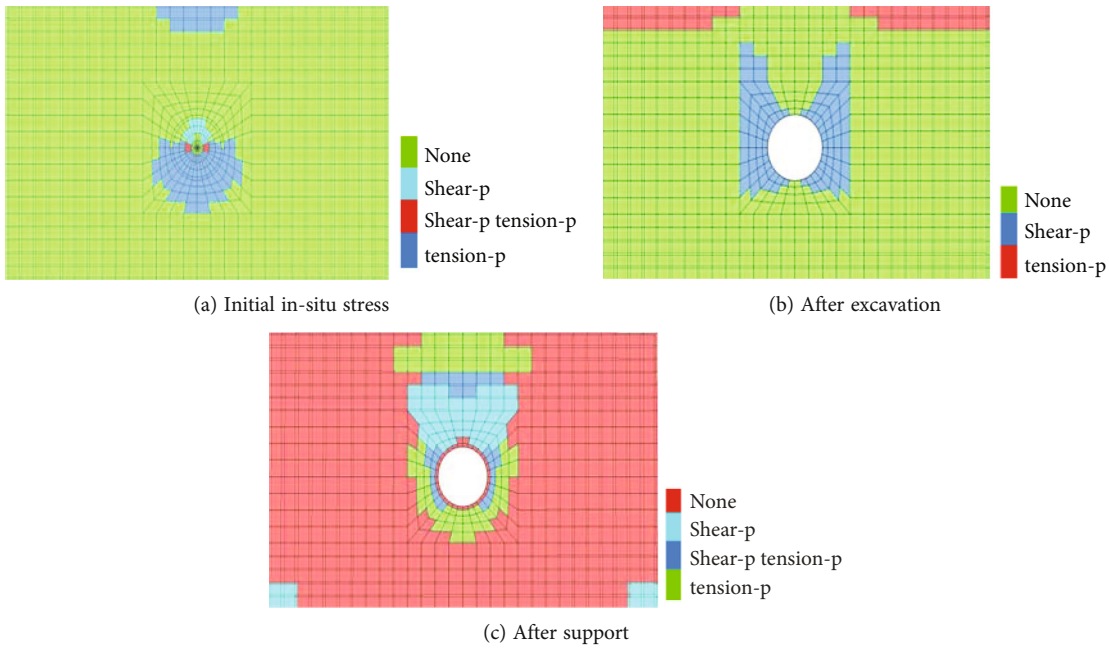

(a) Initial in-situ stress

(b) After excavation

(c) After support

Figure 22: Distribution of plastic zone.

two parts, one around the tunnel and the other near the surface, analyze the distribution of plastic zone after initial in situ stress, excavation, and support, the distribution of plastic zone is shown in Figure 22.

In the original rock stress field, the stratum will be in a stable state. When the tunnel is excavated, the surrounding rock is easy to reach the limit state, resulting in yield and plastic zone. The limit state of tensile stress may also be reached at the top and bottom of the arch, forming a tensile plastic zone. In the spandrel and other parts, the shear stress increases gradually, which is easy to produce shear yield. The appearance of surrounding rock plastic zone can make the stress continuously transfer to the deep part of surrounding rock, and can also deform towards the direction of tunnel and gradually eliminate the stress in the plastic zone. The deformation of tunnel surrounding rock is accompanied by tunnel excavation. Therefore, tunnel construction leads to the plastic state of tunnel surrounding rock. The excavation and construction of tunnel will inevitably produce the phenomenon of plastic zone diffusion, that is, the area of plastic zone is becoming larger and larger. In the initial stress field of the construction gravity field, the plastic zone tensile failure occurs in the upper soil layer, as shown in Figure 22(a). After the excavation of the simulated rough tunnel, the plastic area around the tunnel becomes larger, and the soil layer around the tunnel appears shear failure, as shown in Figure 22(b). After the support, the failure form of the soil around the tunnel is alleviated, and a plastic zone mixed with shear failure, shear, and tension appears, as shown in Figure 22(c). In tunnel construction, the plastic zone mainly appears on the side wall, that is, the plastic zone on the side wall of the tunnel is significantly concentrated, which can be crescent-shaped, ear-shaped, or X-shaped extending towards the deep part of the surrounding rock.

5. Conclusions

(1) Surface deformation and settlement are the interaction and influence of time and space effects. Land subsidence does not occur at one time. Land subsidence occurs in stages, and in each stage, various types of surface movement and deformation usually occur at the same time. With the passage of time, it produces three-dimensional deformation in space, and then changes with the push of the tunnel working face. With the longitudinal development of the tunnel, the surface subsidence trough is also expanding and developing. It can be measured by the maximum settlement and the width coefficient of the settlement tank

(2) The surface deformation caused by urban tunnel construction is related to geological and hydrological conditions, construction methods, and technology. The factors of surface deformation are analyzed by analyzing the deformation mechanism and combined with the evaluation method. It is concluded that the change of soil parameters will cause the change of surface settlement to varying degrees, the existence of groundwater will expand the influence range of surface deformation, and the surface settlement deformation will increase significantly when the in situ stress release of the excavation surface increases. Using the fishbone diagram analysis method, the weight of influencing

factors of surface deformation caused by shield construction is obtained from five aspects: personnel, materials, construction technology, mechanical equipment, and environment

(3) The three-dimensional finite difference numerical simulation software FLAC3D is used to analyze the law of surface deformation and settlement failure caused by tunnel excavation, and the temporal and spatial evolution law of external and internal deformation and failure of rock and soil mass in tunnel excavation is revealed. The rock mass deformation mainly occurs at the arch crown and arch bottom, and most of them are in the state of compressive stress. The stratum settlement at the axis is the largest, and the plastic area on the side wall of the tunnel is significantly concentrated. With the expansion of tunnel excavation scope, the influence area of deformation is increasing. After using concrete lining support, the deformation of rock and soil around the tunnel is reduced and the support stability is enhanced, which strongly verifies the effect of lining support in tunnel stability control

(4) In this paper, theoretical analysis and numerical simulation methods are used to comprehensively study the appearance characteristics, influencing factors, and damage and failure law of surrounding rock instability and deformation caused by tunnel excavation disturbance, which provides an important reference for the study of unloading failure effect and stability control of tunnel excavation rock mass. In the later stage, application research will be carried out in combination with laboratory tests and engineering cases to enrich the research system and make the research conclusions more universal

Data Availability

The data used to support the findings of this study are included within the article.

Conflicts of Interest

The authors declare that they have no conflicts of interest regarding the publication of this paper.

Acknowledgments

This work is supported by the National Natural Science Foundation of China (Grant No. 51904266), Excellent youth project of Hunan Provincial Department of Education (Grant No. 21B0144), and Research project on teaching reform of colleges and universities in Hunan Province in 2020 (Grant No. HNJG-2020-0231).

References

[1] Q. H. Qian, "Welcome the development of urban underground space in my country," *Chinese Journal of Geotechnical Engineering*, vol. 20, no. 1, pp. 112-113, 1998.

[2] R. B. Peck, *Deep Excavations and Tunnelling in Soft Ground*, International society for soil Mechanics and geotechnical engineering, Mexico City, 1969.

[3] Y. Shao, *Land Subsidence and Deformation by Shield Tunnelling Construction of Line 4 in Suzhou Subway*, China University of Mining and Technology, Xuzhou, China, 2016.

[4] Y. Fan, Y. Su, Y. Yuan, and X. P. Yao, "Study on ground settlement law of double-line subway tunnel construction in composite stratum," *Chinese Journal of Underground Space and Engineering*, vol. 16, pp. 762–768, 2020.

[5] J. Jia, J. S. Shi, S. H. Zhou, and K. Wei, "Forecast and analysis of surface settlement of metro station construction by shield tunnel expanding," *Chinese Journal of Rock Mechanics and Engineering*, vol. 32, no. S1, pp. 2883–2890, 2013.

[6] S. K. Sharan, "Exact and approximate solutions for displacements around circular openings in elastic-brittle-plastic Hoek-Brown rock," *International Journal of Rock Mechanics and Mining Sciences*, vol. 42, no. 4, pp. 542–549, 2005.

[7] M. H. Yu, Y. W. Zan, W. Fan, J. Zhao, and Z. Dong, "Advances in strength theory of rock in 20 century—100 years in memory of the Mohr- Coulomb strength theory," *Chinese Journal of Rock Mechanics and Engineering*, vol. 19, no. 5, pp. 545–550, 2000.

[8] G. Lin and Z. Wang, "Strength criterion of concrete considering effects of stress spherical tensor history," *China Civil Engineering Journal*, vol. 35, no. 5, pp. 1–6, 2002.

[9] K. H. Park, B. Tontavanich, and J. G. Lee, "A simple procedure for ground response curve of circular tunnel in elastic- strain softening rock masses," *Tunnelling and Underground Space Technology*, vol. 23, no. 2, pp. 151–159, 2008.

[10] Y. K. Lee and S. Pietruszczak, "A new numerical procedure for elasto-plastic analysis of a circular opening excavated in a strain-softening rock mass," *Tunnelling and Underground Space Technology*, vol. 23, no. 5, pp. 588–599, 2008.

[11] M. Y. Wang, P. X. Fan, Q. H. Qian, and H. J. Deng, "Elasto-plastic model for discontinuous shear deformation of deep rock mass," *Journal of Central South University of Technology*, vol. 18, no. 3, pp. 866–873, 2011.

[12] J. A. Hudson, F. H. Cornet, and R. Christiansson, "ISRM Suggested Methods for rock stress estimation–Part 1: Strategy for rock stress estimation," *International Journal of Rock Mechanics and Mining Sciences*, vol. 40, no. 7-8, pp. 991–998, 2003.

[13] J. Li, M. Y. Wang, P. X. Fan, and C. C. Shi, "Study of loading-unloading states and energy distribution relationship for rock mass," *Rock and Soil Mechanics*, vol. 33, no. S2, pp. 125–132, 2012.

[14] C. Z. Qi and Q. H. Qian, *Basic Problems of Dynamic Deformation and Failure of Rock Mass*, Beijing, Science Press, 2009.

[15] H. Wu, B. Dai, L. Cheng, R. Lu, G. Zhao, and W. Liang, "Experimental study of dynamic mechanical response and energy dissipation of rock having a circular opening under impact loading," *Mining, Metallurgy & Exploration*, vol. 38, no. 2, pp. 1111–1124, 2021.

[16] X. L. Li, S. J. Chen, S. M. Liu, and Z. H. Li, "AE waveform characteristics of rock mass under uniaxial loading based on Hilbert-Huang transform," *Journal of Central South University*, vol. 28, no. 6, pp. 1843–1856, 2021.

[17] G. Wei, "Research on theoretical calculation of long-term ground settlement caused by shield tunneling," *Chinese Journal of Rock Mechanics and Engineering*, vol. 27, no. S1, pp. 2960–2966, 2008.

[18] D. M. Zhang, H. W. Huang, and J. Yang, "Influence of partial drainage of linings on long-term surface settlement over tunnels in soft soils," *Chinese Journal of Geotechnical Engineering*, vol. 27, no. 12, pp. 1430–1436, 2005.

[19] Q. Fang, J. M. Du, Z. J. Wang, and L. I. U. Xiang, "Model experimental study on stratum deformation of shield tunnelling in sand," *China Journal of Highway and Transport*, vol. 34, no. 5, pp. 135–143, 2021.

[20] K. W. Ding and M. Wang, "Study on the influence of shallow subsurface excavation method transformation on ground settlement," *Chinese Journal of Underground Space and Engineering*, vol. 15, no. S1, pp. 225–230, 2019.

[21] Q. X. Xu, B. Liu, and M. Jin, "Simulation of the geological stability and the osmotic characteristics as subway tunnel crossing rivers," *Journal of Safety Science and Technology*, vol. 3, no. 1, pp. 62–65, 2007.

[22] X. L. Lv, Y. C. Zhao, and J. T. Cai, "Numerical simulation of ground subsidence induced by shield tunnel construction disturbance in water-rich sandy stratum," *Modern Tunnel Technology*, vol. 57, no. 5, pp. 104–109, 2020.

[23] Z. S. Wang and M. S. Wang, "Effects of shield-driven tunneling on the safety of adjacent buildings and its countermeasures," *China Safety Science Journal*, vol. 12, no. 2, pp. 48–52, 2002.

[24] C. Z. Yang, Y. J. Wu, W. Wang, and Y. Q. Tang, "Analysis on influence of spacial effect on excavation of soft rock tunnel with large cross section," *Chinese Journal of Underground Space and Engineering*, vol. 17, no. 2, pp. 511–519, 2021.